MINERALOGICAL AND GEOCHEMICAL FEATURES OF DEPOSITS IN THE SOUTHEASTERN TRANSBAIKALIA FOR LOCAL FORECAST OF URANIUM ORE

Andrey A. Chernikov
Fersman Mineralogical Museum, RAS, Moscow, mineral@fmm.ru, cher@fmm.ru
Victor T. Dubinchuk, Anatoly E. Tolkachev, Natalia I. Chistyakova, and Georgy N. Nechelyustov
All-Russia Institute of Mineral Resources, Moscow, vims@df.ru

A.A. Chernikov discovered the uranium-molybdenum hydrochemical anomaly in the southern Argun region (southeastern Transbaikalia) that had been forcible argument for geological substantiation to renew research and exploration for uranium in this region. This anomaly is important to understand a state of supergene zone of uranium deposits with leached near-surface oxidired zone in the region. The Strel'tsovsk-Antei largest uranium deposits in Russia (Laverov *et al.*, 1991, 1992) are characterized by great vertical extension (2.7 km) of ore mineralization and variation of ore mineralogy, mineralogy of metasomatic and host rocks downward (Ishchukova and Modnikov, 1991; Andreeva *et al.*, 1996; Chernikov, 2006/2007). Chernyshov and Golobev (1996) reported and we confirmed in this study that massive pitchblende ore was deposited within interval 134 – 136 (~150) Ma. Isotopic age of "protore" is 250 – 260 (~300) Ma; age of Th-bearing uraninite is ~500 Ma and older. New data indicated that uranium (IV) oxides and silicates, including coffinite, uranium titanates, and brannerite, in ore of the Antei deposit are young, from zero to few Ma. Exclusively very young uranium (IV) silicates and titanates are observed at lower levels of the Anntei deposit. These mineral precipitated from meteoric water infiltrated from surface into deep levels of the deposit. The basic level of karst and fracture rocks can be probable outflow area of meteoric water at the Argun deposit. Distribution of oxygen and carbon isotopes in the Argun and Antei structural clusters confirms the main role of meteoric solution to form various minerals at the uranium deposits; this is important for revealing additional exploration and estimation criteria for these deposits. Large uranium accumulations are predicted to the northward of the Strel'tsovsk structure.

1 table, 7 figures, 22 references.
Keywords: uranium ores, uranium silicates, uranium titanates, oxidized zone of uranium deposits, deep-seated hypergenesis, Argun deposit, Strel'tsovsk-Antei deposits.

Introduction

Mineralogical and geochemical study of deposits and occurrences carried out by the authors since 1957 in the southern Argun region, the southeastern Transbaikalia have revealed hydrochemical U-Mo anomaly overcapping the Strel'tsovsk volcano-tectonic structure and host basement rocks (Fig. 1) (Chernikov *et al.*, 2007a, 2007b, 2008). At background Mo and U of $n \cdot 10^{-7}$ to $1 \cdot 10^{-6}$ g/l in waters circulating in host rocks, the great anomaly with $1 \cdot 10^{-5}$ – $n \cdot 10^{-4}$ g/l U and Mo was found in subsurface water of the Strel'tsovsk structure, water of the Urulyungui river and Kisly (Acid) spring in the northern side of the East Urulyungui depression. Concentration of uranium in water of the Urulyungui river downstream of settlement Dosatui is not lower than $n \cdot 10^{-5}$ g/l.

These results were forcible argument for substantiation to renew research and geological exploration for uranium in this region in 1962, which had been terminated in 1957. In addition, the results obtained are important to understand a state of supergene zone in the region and contents of uranium and molybdenum in water combined with below new data can be applied to elaboration of research and geological exploration guids of uranium deposits and their local forecast.

Mineralogical and geochemical features of oxidized zone and unoxidized ore of the deposits

The near-surface oxidized zone of uranium deposits in the Southern Argun region is pronounced and highly leached along some well permeable structures down to

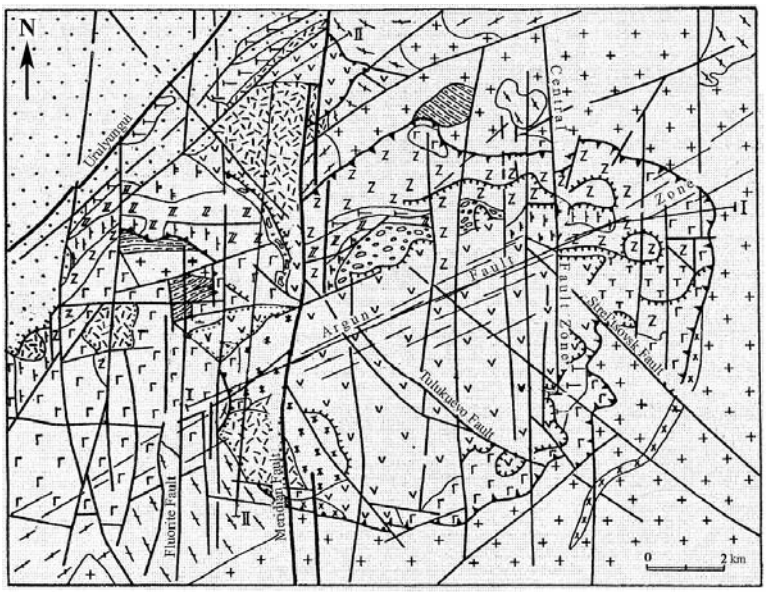

Fig. 1. Geological scheme of the Strel'tsovsk volcano-tectonic structure, after Ishchukova et al. (2005).

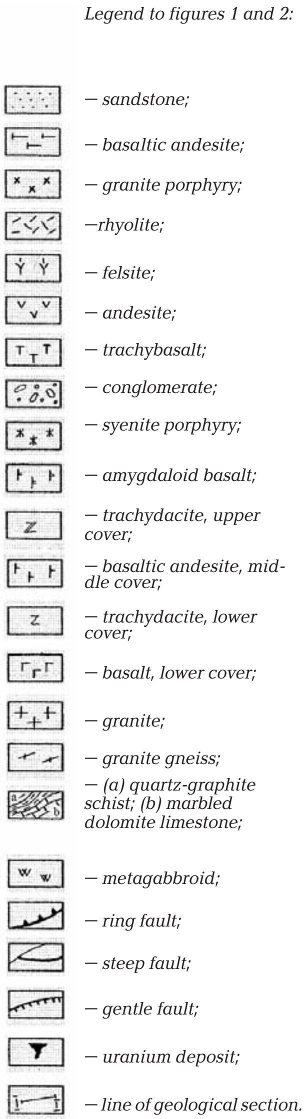

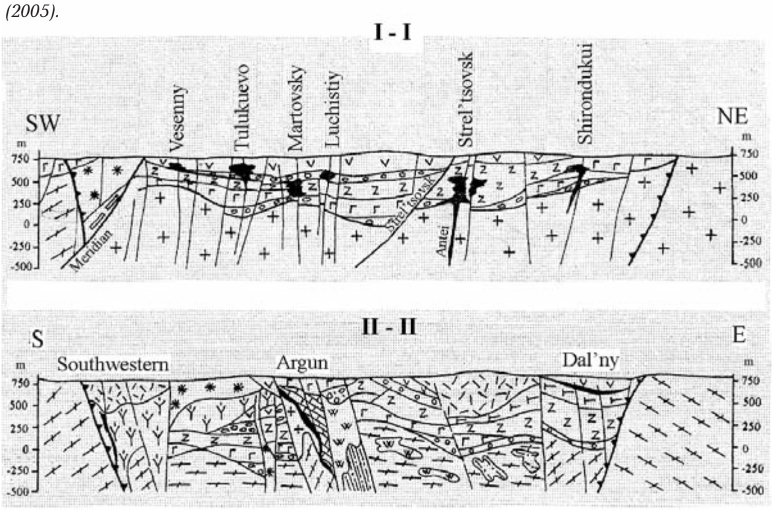

Fig. 2. Geological sections along lines I — I and II — II.

300 — 500 m below surface, where it gradually turns to the deep-seated leached supergene zone. In oxidized zones, uranium was leached from both ore and host rocks. Present uranium content in such zones is hundreds and locally thousand times lower than primary concentration calculated from ^{206}Pb radiogenic additive for age of 150 Ma. As a result of these, all economic orebodies and host rocks enriched in uranium are exposed at the depth of tens to hundreds meters below surface while ground water form aforementioned large hydrochemical U-Mo anomaly.

Mainly iron and manganese oxides and hydroxides with uranium background $2 \cdot 5 \cdot 10^{-4}$%, rarely $n \cdot 10^{-3}$%, sometimes higher occur in the near-surface oxidized zone of most deposits (about 20 deposits have been discovered since 1962). Oxidized zones with economic uranium content were preserved only at the Tulukuevo, Luchistoe (Fig. 2) and Krasny Kamen′ (out of section) deposits. These oxidized zones exposed at the depth of few tens meters below surface are blind and overlain by barren or weakly radioactive rocks.

The largest Russia's uranium deposits (Laverov *et al.*, 1991, 1992) Streltsovsk and Antei (the former is hosted in volcanic rocks of the structure, the latter, in basement granites) are characterized by the absence of economic uranium concentration in the near-surface oxidized zone, great vertical extension of orebodies (2.7 km) (Fig. 3), change of the mineralogy of ores, of metasomatic wall-rocks and of host rocks in the vertical geological section (Ishcukova *et al.*, 1991, 2005; Andreeva *et al.*, 1996; Chernikov, 2006/2007). Chernyshov and Golubev (1996) reported and we confirmed that according to U—Pb age of massive nasturan ore hosted in Mesozoic volcanic rocks at the Strel′vovsk deposit ranges from 134 to 136 (or ~150) Ma. Isotopic age of "protoores" is 250—260 (~300) Ma; age of Th-bearing uraninite is ~500 Ma; and probably, age of disseminated uraninite is more than 500 Ma. However, we documented various intermediate ages and nearly present minerals by dating our samples and samples by I.S. Modnikov and I.V. Sycheva (Table 1).

Hypotheticaly, disseminated uraninite is not identified. Therefore, the mineral assemblages dated more than 500 Ma can not be characterized and determined only by excess radiogenic lead. U-Mo mineralization of ~500 is found in basement rocks between Argun and Tulukuevo depressions as well as in Tulukuevo depression basement between the Argun and Tulukuevo deposits is of ~500 Ma. Xenoliths of Proterozoic albitized amphibolite and schist containing uraninite-molybdenite mineralization were found in the Paleozoic granitoids at these deposits. Andradite, titanite, allanite, phlogopite, ilmenite, apatite, and zircon are characteristic minerals of these albitized rocks. Previously, uraninite-

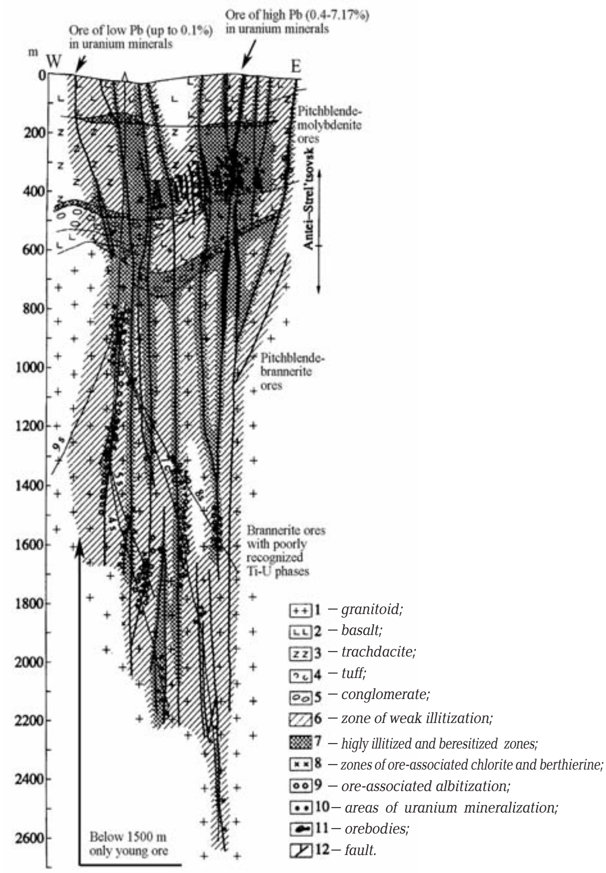

Fig. 3. Sketch geological section of the Strel′tsovsk-Antei deposits with distribution of wall-rock alteration, modified after Andreeva et al. (1996), with the authors additions on ore geochemistry and mineralogy.

molybdenite mineralization was studied by K.V. Skvortsova and N.S. Trofimov. Coarse-flake (up to 2 mm) hexagonal (2H) molybdenite is distinguished by low concentration of trace elements (0.0n % Fe, Cu, Pb, Zn; 0.00n % Sb, Bi); the unit-cell dimensions are a_0 = 0.315 nm, c_0 = 1.229 nm. Th-bearing uraninite occasionally is replaced by coffinite (Fig. 4) that results in Si in composition of the mineral. The composition is as follows, wt. %: 81.33—82.35 UO_2, 0.0—0.12 Y_2O_3, 0.36—0.38 ZrO_2, 10.18—10.68 ThO_2, 5.38—6.07 PbO, 0.45—0.88 CaO, 0.0—1.81 SiO_2; total is 99.65—99.94.

Nasturan from the Dosatui occurrence may be an example of the 300 Ma "protoore". Its composition is as follows, wt. %:

Table 1. **Chemical composition of uranium silicates and titanates of the Antei uranium deposit, wt. %**

No	Dept, m	Major mineral	UO_2	TiO_2	CaO	ThO_2	PbO	ZrO_2	Fe_2O_3	SiO_2	Total
1	210	Brannerite	51.13	38.45	4.93	<0.01	1.54	< 0.01	Bdl	2.76	98.81
2	230	Brannerite	58.81	35.44	2.05	<0.01	1.22	0.33	1.02	0.36	99.25
3	230	Si titanate	57.4	13.10	1.0	<0.01	0.00	Bdl	1.06	10.10	82.66
4	230	Si titanate	56.60	13.9	1.9	<0.01	0.60	Bdl	1.22	9.0	83.22
5	230	Si Brannerite	54.60	18.2	2.00	Bdl	0.50	<0.01	2.5	5.29	83.09
6	230	Si Brannerite	57.80	14.00	1.75	Bdl	0.20	<0.01	1.99	10.10	85.84
7	230	Coffinite	55.40	Bdl	3.0	Bdl	0.00	Bdl	3.56	21.6	83.56
8	298	Brannerite	54.1	32.4	1.53	<0.01–	0.8	2.2	1.1	1.49	93.62
9	298	Brannerite	53.4	33.3	1.79	Bdl	0.4	2.4	1.1	1.16	93.55
10	448	Silicate U	54.46	0.11	1.86	Bdl	<0.15	0.15	0.87	10.39	77.84
11	448	Silicate U	55.65	0.12	1.73	Bdl	<0.15	9.28	0.58	9.44	76.80
12	448	Coffinite	65.42	0.46	2.10	Bdl	<0.15	0.43	0.47	18.66	87.54
13	448	Coffinite	58.24	1.63	1.68	Bdl	<0.15	1.78	1.63	18.99	83.95
14	558	Silicate U	74.54	0.31	2.39	Bdl	<0.15	1.15	0.48	12.10	90.97
15	558	Ti-Silicate U	54.80	25.47	2.04	Bdl	<0.15	2.03	0.83	10.82	95.99
16	558	Ti-Silicate U	47.63	23.93	2.02	Bdl	<0.15	2.47	0.81	10.55	87.48
17	558	U oxide Ti	14.02	64.72	0.87	Bdl	<0.15	1.58	5.78	3.77	90.74
18	910	Si-Zr titanate	60.7–	21.99 –	0.98–	Bdl	0.00–	2.51–	1.58–	6.02–	91.35–
		U. 7 analyses	17.28	50.94	1.83		0.83	8.41	4.57	11.91	93.74
19	910	Si oxide U.	69.23–	0.00–	1.22–	Bdl	0.00–	0.35–	0.10–	11.43–	92.30–
		6 analyses	74.71	0.45	2.50		0.39	1.79	0.57	14.75	95.17
20	1260	Si titanate	36.49	46.55	1.46	2.08	0.78	0.89	0.35	7.21	95.81
21	1573	Silicate U	59.2	0.1	1.8	<0.5	<0.1	1.4	0.3	13.0	91.80
22	1590	Brannerite	50.1	35.3	1.57	Bdl	0.03	1.1	1.8	2.5	94.80
23	1590	Brannerite	54.8	33.4	2.18	Bdl	0.03	1.4	2.5	2.5	97.01
24	1700	Si Brannerite	41.48	32.6	2.7	0.34	0.2	Bdl	Bdl	6.88	86.25
25	1700	Brannerite	45.65	35.1	3.5	<0.3	0.1	Bdl	Bdl	2.22	89.36
26	1718	Coffinite	61.4	<0.1	1.5	0.5	<0.1	0.5	Bdl	16.7	91.20
27	1718	Si Brannerite	43.64	33.0	2.94	1.12	<0.15	0.6	Bdl	5.85	89.92
28	1718	Brannerite	49.75	35.2	3.01	1.2	0.15	0.4	Bdl	0.3	92.45
29	1979	Coffinite	50.3	0.1	1.4	Bdl	<0.1	1.4	1.0	19.7	82.40
30	2020	Brannerite	42.5	33.4	2.3	Bdl	0.03	0.7	Bdl	6.6	86.75
31	2509	Coffinite	61.5	<0.1	0.5	<0.5	<0.1	Bdl	Bdl	18.4	95.40
32	2509	Brannerite	48.28	32.9	2.3	Bdl	<0.1	Bdl	Bdl	0.7–4.5	90.04

Notes: An JXA-8100 Jeol electron microprobe operating at 20 kV and current 2 nA. The following analytical lines were used ULα, TiKα, CaKα, Th Lα, PbLα, Zr Lα, FeKα, u SiKα. Standards were: UO_2, TiO_2, diopside (Ca and Si), ThO_2 (Th), PbTe (Pb), ZrO_2 (Zr), almandine (Fe).

Samples 1 and 2 characterize the lower levels of the Strel'tsovsk deposit. In addition to oxidess listed in the Table, the following species were detected, wt. %: 0.0n–2.5 Al_2O_3, up to 3 P_2O_5, up to 0.65 V_2O_3, up to 1.4 WO_3; 0.1–8.9 Y_2O_3 in samples 21, 23, 25, 26, 27, 28, and 31; 0.7 Nb_2O_3 in sample 29. The major mineral phases were named according to relation of oxides.

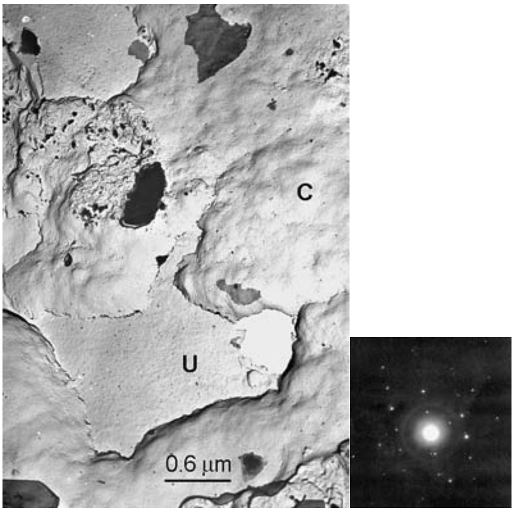

Fig. 4. Replica extraction. Colloform coffinite (C) replaces uraninite (U). Inset: Microdiffraction pattern of coffinite.

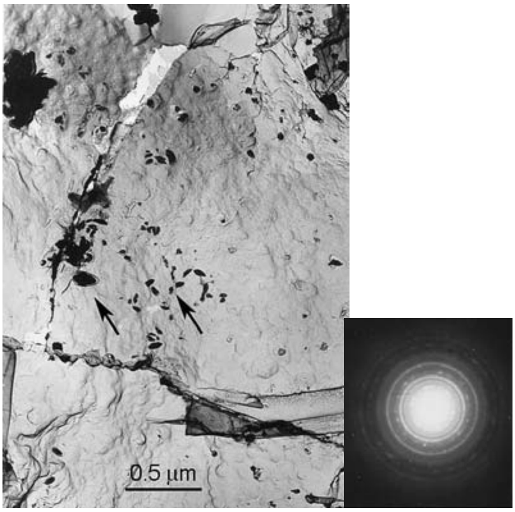

Fig. 5. Replica extraction. Pitchblende fills the whole visible field. Extracted particles are coffinite (arrows). Inset: Microdiffraction pattern of coffinite.

– 92.10 – 94.02 U_3O_8, 0.25 – 0.32 SiO_2, 0.38 – 0.76 CaO, 0.41 – 0.68 Fe_2O_3, 3.36 – 3.45 PbO, 1.32 – 1.35 Y_2O_3; total is 98.52 – 98.54. Sufficiently high Pb, Y, and absence of Th are characteristic features of the mineral.

Massive rich ores of the Strel'tsovsk deposit with age of ~150 Ma are mainly pitchblende with insignificant coffinite (Fig. 5) and brannerite, as well as nasturan with molybdenite (+femolite) and coffinite. Previously, many mineralogists and in the first place, I.V. Mel'nikov, V.P. Rogova, M.V. Vampilov, K.V. Skvortsova, Yu.M. Dymkov, and N.S. Trofimov examined pitchblende. At least four reniform generations of the mineral are recognized. These generations differ in reflectance (from 14 to 16%), size (course-, medium-, and fine-reniform), and associated minerals (coffinite, brannerite, quartz, pyrite, molybdenite, illite, montmorillonite, and Fe-rich chlorite and other minerals).

In addition to uranium, Ti, Zr, Fe, Pb, Ca, Si, occasional Mg, Al, Y, and S rarely other chemical elements were detected by numerous electron microprobe analyses.

Twenty analyses show variable composition of the mineral, wt. %: 73.10 – 94.82 UO_2, 0.10 – 4.03 TiO_2, 0.48 – 5.20 Zr_2O_3, trace – 1.91 Fe_2O_3, 0.42 – 7.17 PbO, 1.10 – 3.32 CaO, 0.15 – 3.46 SiO_2, locally up to 1.58 SO_3, 0.21 ThO_2, 0.11 Y_2O_3, up to 0.04 Sb_2O_3; total is 91.34 – 99.63.

According to X-ray diffraction data, molybdenite from these ores is a mixture of hexagonal and rhombic modifications (2H + 3R). Semiquantitative spectral analyses of this molybdenite revealed admixture of Fe (0.2 – 2.0 %), Pb, Sb, As, Tl (0.001 – 0.1 %), and locally Ag (0.000n %). These ores also contain Fe-rich molybdenite (femolite) and rare jordisite, X-ray amorphous molybdenum disulfide. Number of molybdenum minerals in the ores decreases downward, whereas content of coffinite and transitional uranium silicate phases increases.

Significant amount of coffinite and transitional silicate mineral phases occurs at the lower levels of the Strel'tsovsk deposit, in the margins of vein pitchblende-molybdenite ore and in stratiform ore of the Dal'nee and Yubeleinoe deposits (Fig. 2, section along line II – II). These phases, as rule, are hydrated, poor crystallized or X-ray amorphous, and recently are called uranium-bearing gels (Dymkov *et al.*, 2003; Aleshin *et al.*, 2006). In most cases, these are nanoscale segregations of coffinite and complex silicate phases transitional from titanates simi-

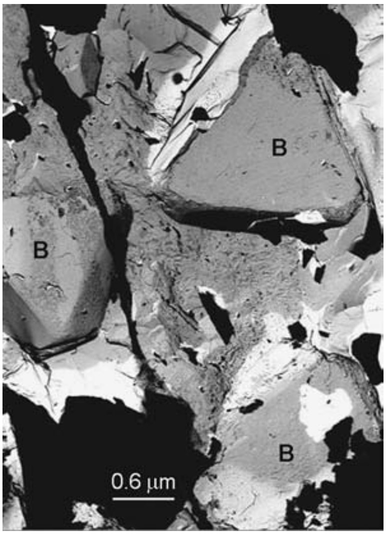

Fig. 6. Replica extraction. Metamict crystals of brannerite (B) in pitchblenede (gray field).

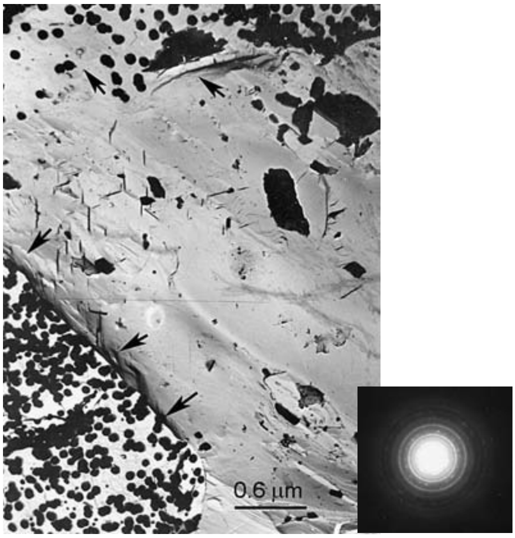

Fig. 7. Replica extraction. Rounded segregations of uranium oxide (arrows) on the surface of quartz grain. Inset: Microdiffraction pattern of uranium oxide.

lar to rutile, ilmenite or titanomagnetite (?) to brannerite (Fig. 6) or uranium oxides (Fig. 7). In addition to U and Si, their formation is accompanied with introduction of zirconium and calcium in deposition areas. In this case, content of PbO in many these phases is lower than hundredths percent indicating their young (near present) geological age. We have composition one of such phases determined with an electron microprobe, wt. %: 61.4 UO_2, 16.7 SiO_2, 0.7 Al_2O_3, 1.5 CaO, 0.5 ThO_2, 0.5 ZrO_2, 1.5 P_2O_5, and 1.4 Y_2O_3 that corresponds to formula of coffinite $U(SiO_4)_{1-x}(OH)_{4x}$. The mineral is sufficiently well crystallized and its unit-cell dimensions are: a_0 = 0.6960 nm, c_0 = 0.6288 nm (±0.0002 nm) that is consistent with reference data of coffinite. X-ray powder diffraction study of the other uranium silicate was failed.

Many researchers studied in detail brannerite from the Strel'tsovsk deposit. According to analytical electron microscopy (Ivanova *et al.*, 1982), natural unheated brannerite from this deposit is identical to its synthetic analogue $U[TiO_3]_2$. However, we identified various transitional varieties from brannerite to coffinite and nasturan in the ore of the Strel'tsovsk deposit.

At the Antei deposit, amount of uranium silicates and titanates in the ore exposed in the basement granite significantly increases. Uranium titanates (more precise determination is impossible) and less abundant brannerite mainly occur at the lower levels; according to PbO content, identified uranium silicate and titanate minerals at the deep levels (below 1500 m) are of young geological age (Table 1) indicating their recent precipitation from meteoric water infiltrated from the surface to deep levels of the deposit. Basic level of karsting and fracturing at the Argun deposit can be outflow area of meteoric solution in this district (Fig. 2). Distribution of oxygen and carbon isotopes confirms the major role of meteoric water to form gangue minerals (calcite and dolomite) of ore zones in the Antei and Argun structural clusters. Mean $\gamma^{13}C$ and $\gamma^{18}O$ values of gangue minerals in the Argun cluster are −0.68‰ and +3.25‰, respectively; these values in the Antei cluster are −1.46‰ and +10.0‰, respectively. These values show minor role of organic matter to form gangue minerals in both clusters. According to carbon and oxygen isotopic study, in the Antei cluster, minerals were probably formed at decreasing temperature when ore structures pinched out.

Conclusion on meteoric source of mineralizing fluids is consistent with previous determined oxygen and hydrogen isotopic composition of sericite and illite from altered wall rocks (Andreeva and Golovin, 1998). As previously suggested, alkali thermal present deep water (40 – 40.5°C) interacts with granite of tectonic zones of neighboring Dauriya crest uprising to form zeolites and clay minerals (Chernikov, 2001). The same minerals are observed in some ores of the Strel'tsovsk structure, therefore they can be formed under the similar conditions. Oxygen and hydrogen isotopic study of waters (thermal up to 80 – 100°C and cold) in Baikal hydromineral area indicated that δD and $\delta^{18}0$ of thermal water of Transbaikalia correspond to meteoric values. As previously reported (Chernikov *et al.*, 2007), all these data testify to important role of meteoric supergene as well as thermal or hydrothermal, as usually they are called, water to form variable minerals and ores. This allows supplementing exploration and prospecting criteria for large deposits (Chernikov, 2006/2007). The major predicted criteria (Ishchukova *et al.*, 2005) allowing to determine the scale of deposits in volcano-tectonic structures, basement rocks, and sedimentary cover should be added by: (1) near-surface zones of leached uranium in the rocks of predicted area; (2) high concentration of uranium and accompanied elements in streams and underground water of this area; (3) occurrence of uranium ore in stratified sediments of volcano-tectonic structures; (4) karst-forming rocks (limestone, marble); (5) oxidation zones of occurrences in basement and volcanic cover are significantly leached and depleted in uranium; and (6) polygene uranium mineralization of variable age.

Conclusion

Strongly leached oxidized zones, significant concentration of uranium minerals precipitated from meteoric water, high uranium content in mineral springs and water of the Urulyungui river downstream, and presents of stratiform deposits, for example Dalnee allow to predict the formation of large uranium mineralization first of all northward of the Strel'tsovsk structure, where these aforementioned prospected criteria are pronounced: 1) in the basement rocks along the Uryulungui fault zone on spletting and cut structures; 2) in basement rocks of the northern side of the East Uryulungui depression; 3) in sediments of the East Uryulungui depression especially in water-permeable beds enriched in organic matter.

Considering the perspective of increasing uranium development in Transbaikalia, B.N. Khomentovsky *et al.* (2000) indicated that stratiform deposits hosted in the Jurassic to Cretaceous sediments of the Olovsky and Urulyngui districts and deposits hosted in the Cenozoic sediments of the Vitim, South Vitim, and Eravnensky district with the Shilka and Dzhida promising areas are the major ore objects of the region. It also follows from the data reported by L.P. Ishchukova (2000) and studies of economic types of uranium deposits as well as performed by G.A. Mashkovtsev *et al.* (1998).

And finally, it should me noted that the notion "deep-seated hypergenesis" was completely revealed by F.V. Chukhrov (1955), who called it "deep-seated weathering". From that time on and as follows from this study, understanding of deep-seated hypergenesis has been broadened. In addition to preparation of weathering profile as reported by F.V. Chukhrov, it was established that deep-seated hypergenesis plays inportant role to form various types of ores, among which there are large and superlarge mineral deposits. Mineralogical and geochemical features of such deposits are important to elaborate their new prospective and appraisal criteria, local predicted ore, and increasing reserves of strategic raw.

References

Aleshin A.P., Andreeva O.V., Velichkin V.I. et al. Deposits of the Strel'tsovsk ore field and Kurku // Large and superlarge mineral deposits. Moscow: IGEM. **2006**. V. 2. P. 299–341. (In Russian.)

Andreeva O.V., Aleshin A.P., and Golovin V.A. Vertical zonality of wall rock alterations at the Antei-Srel'tsovsk uranium deposit, Eastern Transbaikal region, Russia // Geol. Ore Dep. **1996**. V. 38 (5). P. 353–366. (In Russian.)

Andreeva O.V. and Golovin V.A. Metasomatic processes at uranium deposits of Tulukuev caldera, Eastern Transbaikal region, Russia // Geol. Ore Dep. **1998**. V. 40 (3). P. 184–196. (In Russian.)

Chernikov A.A. Deep-seated hypergenesis, mineral and ore formation. Moscow: Fersman Mineralogical Museum. **2001**. 100 p. (In Russian.)

Chernikov A.A. Mineralogical features of uranium ores, large and superlarge deposits of Russia and adjacent countries // Global Tectonics and Metallogeny. **2006/2007**. V. 9 (1–4). P. 21–30.

Chernikov A.A., Tolkachev A.E., Chistyakova N.I., and Nechelustov G.N. Variation of mineralogy and age of uranium minerals along vertical section of the Strel'tsovsk-Antei deposits, eastern Transbaikalia // Proc. Sci. Conf. devoted to Prof. F. I. Vol'fson. Moscow: IGEM. **2007**. P. 223–225. (In Russian.)

Chernikov A.A., Tolkachev A.E., Chistyakova N.I. et al. Role of mineralogical and geochemical features of deposits located in the Strel'tsovsk volcano-tectonic structure, eastern Transbaikalia in local predicted mineralization // Problems of geology ore deposits, mineralogy, petrology, and geochemistry. Proc. Sci. Conf. Moscow: IGEM. **2008**. P. 224–227. (In Russian.)

Chernikov A.A., Tolkachev A.E., Kostikov A.T., Chistyakova N.I., and Nechelustov G.N. Discovery of young minerals (according to U-Pb dating) from the deep levels of Strel`tsovsk-Antei deposit (South-East Transbaikal, Russia) based on the specimens from Fersman Mineralogical Museum and VIMS // IV Inter. Symp. Sofia, Bulgaria. Abstracts. **2007**. P. 6.

Chernyshev I.V. and Golubev V.N. The Strel'tsovskoe deposit, Eastern Transbaikalia: Isotope dating of mineralization in Russia's largest uranium deposit // Geochem. Inter. **1996**. V. 34 (10). P. 834–846. (In Russian.)

Chukhrov F.V. Colloids in the Earth's crust. Moscow: AN SSSR Publ. **1955**. 672 p. (In Russian.)

Dymkov Yu.M., Doinikova O.A., and Volkov N.I. Finding of U-Fe-Zr-Ti-S-P gel at the exogenic epigenetic Khokhlovskoe uranium deposit, southern Transural region // Geochem. Int. **2003**. V. 41 (11). P. 1126–1133. (In Russian.)

Ishchukova L.P. Transbaikalia on the largest uranium provinces in Russia // Razvedka i Okhrana Nedr. **2000**. No 1. P. 54–58. (In Russian.)

Ishchukova L.P., Ashikhmin A.A., Konstantinov A.K. et al. Uranium desposits in volcano-tectonic structures. Moscow: All-Russia Institute of Mineral Resources Publ. **2005**. 212 p. (In Russian.)

Ishchukova L.P., Modnikov I.S., and Sychov I.V. Uranium ore-forming systems of continental volcanic regions // Geol. Ore. Dep. **1991**. V. 33 (3). P. 16–25. (In Russian.)

Ivanova O.A., Mel'nikov I.V., Gorshkov A.I., and Vampilov M.V. Brannerite: evidence from analytical electron microscopy // Izv. AN SSSR. Ser. Geol. **1982**. No 2. P. 63–72. (In Russian.)

Khomentovsky B.N., Ovseichuk V.A., and Shchukin S.I. Prospects of increasing mining of uranium in Transbaikalia // Razvedka i Okhrana Nedr. **2000**. No 1. P. 28–30. (In Russian.)

Laverov N.P., Velichkin V.I., and Shumilin M.V. Uranium deposits of the CIS: the main economic genetic types and their distribution // Geol. Ore Dep. **1992**. V. 34 (2). P. 3–18. (In Russian.)

Laverov N.P., Velichkin V.I., Vetrov V.I. et al. Uranium base of the USSR. Moscow: AN SSSR Publ. **1991**. 71 p. (In Russian.)

Mashkovtsev G.A., Kislyakov Ya.M., Miguta A.K. et al. Economic genetic types of uranium deposits // Otechestv. Geol. **1998**. No 4. P. 13–20. (In Russian.)

Pinneker E.V., Kustov Yu.I., Kalashnikov E.B. et al. Geochemistry of mineral therapeutic waters in Transbaikalia // Otechestv. Geol. **1996**. No 1. P. 42–48. (In Russian.)